Earth and Planetary Science Letters 381 (2013) 1–11

Contents lists available at ScienceDirect

Earth and Planetary Science Letters

www.elsevier.com/locate/epsl

Seismic attenuation beneath Europe and the North Atlantic: Implications for water in the mantle

Hejun Zhu [a,*], Ebru Bozdağ [a], Thomas S. Duffy [a], Jeroen Tromp [a,b]

[a] Department of Geosciences, Princeton University, Princeton, NJ, USA
[b] Program in Applied & Computational Mathematics, Princeton University, Princeton, NJ, USA

ARTICLE INFO

Article history:
Received 17 June 2013
Received in revised form 12 August 2013
Accepted 13 August 2013
Available online 11 September 2013
Editor: P. Shearer

Keywords:
adjoint tomography
seismic attenuation
the mantle transition zone
subduction zones
water transport

ABSTRACT

It is well known that anelasticity has significant effects on the propagation of seismic waves, as manifested by physical dispersion and dissipation. Investigations of anelasticity provide complementary constraints on the physical properties of Earth materials, but — contrary to imaging with elastic waves — progress in mapping Earth's anelasticity has been relatively slow, and there is only limited agreement between different studies or methodologies. Here, within the framework of adjoint tomography, we use frequency-dependent phase and amplitude anomalies between observed and simulated seismograms to simultaneously constrain upper mantle wavespeeds and attenuation beneath the European continent and the North Atlantic Ocean. In the sea-floor spreading environment beneath the North Atlantic, we find enhanced attenuation in the asthenosphere and within the mantle transition zone (MTZ). In subduction zone settings, for example beneath the Hellenic arc, elevated attenuation is observed along the top of the subducting slab down to the MTZ. No prominent reductions in wavespeeds are correlated with these distinct attenuation features, suggesting that non-thermal effects may play an important role in these environments. A plausible explanation invokes the transport of water into the deep Earth by relatively cold subducting slabs, leading to a hydrated MTZ, as previously suggested by mineral physics and geodynamics studies.

1. Introduction

Current knowledge of heterogeneities in the Earth's mantle primarily comes from tomographic studies of elastic wavespeeds. Based on traveltimes of body waves, dispersion of surface waves, and splitting of free oscillations, seismologists routinely estimate lateral variations in elastic wavespeeds within the Earth's interior (e.g., Woodhouse and Dziewonski, 1984; Van der Hilst et al., 1997; Romanowicz, 2003; Montelli et al., 2004). However, Earth materials exhibit anelasticity, an energy dissipation mechanism that manifests itself in the form of physical dispersion and attenuation of seismic waves (Liu et al., 1976). 3D maps of lateral variations in anelastic attenuation provide complementary constraints on variations in temperature, water content, partial melt, and composition (Karato, 2003). For instance, guided by mineral physics experiments, Shito et al. (2006) combined tomographic images of elastic wavespeeds and anelastic attenuation to estimate 3D variations in temperature, water content and other parameters, such as major element chemistry and melt fraction.

There is no consensus among seismologists on how the effects of attenuation should be quantified and measured. Contrary to wavespeed models, existing global models of attenuation exhibit limited agreement, e.g., Romanowicz (1995), Gung and Romanowicz (2004), Dalton et al. (2008). In contrast to body-wave traveltimes or surface-wave dispersion, which are solely governed by seismic wavespeeds, seismic wave amplitudes are affected by a host of competing factors besides anelastic attenuation, such as earthquake magnitudes and radiation patterns, elastic focusing and defocusing, and scattering (Ruan and Zhou, 2010, 2012).

We have developed a new tomographic technique, called "adjoint tomography" (Tromp et al., 2005; Tape et al., 2007, 2009, 2010; Liu and Tromp, 2008; Zhu et al., 2012), to simultaneously constrain elastic wavespeeds and anelastic attenuation. Frequency-dependent phase and amplitude differences between observed and simulated seismograms (Laske and Masters, 1996; Ekström et al., 1997; Zhou et al., 2004) are simultaneously considered in the inversion in order to ensure a consistent treatment between anelastic attenuation and elastic focusing/defocusing (Billien et al., 2000). Synthetic seismograms are computed based on a spectral-element method (Komatitsch and Tromp, 1999; Peter et al., 2011), and Fréchet derivatives with respect to the model parameters are numerically calculated in a 3D background model based on adjoint methods (Lailly, 1983; Tarantola, 1984; Tromp et al., 2005; Liu and Tromp, 2008). Body and surface waves recorded in three-component seismograms are combined to simultaneously constrain

* Corresponding author.
E-mail address: hejunzhu@princeton.edu (H. Zhu).

0012-821X/$ – see front matter
http://dx.doi.org/10.1016/j.epsl.2013.08.030

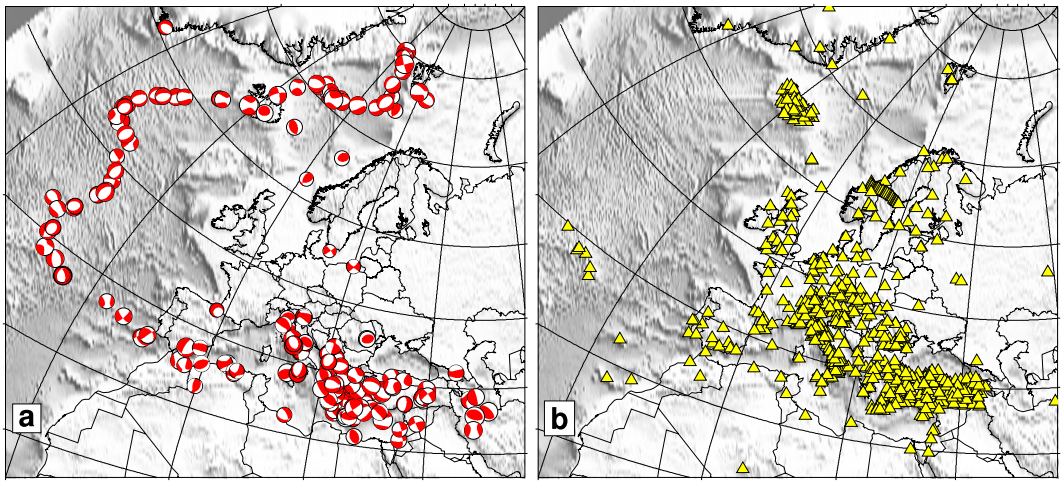

Fig. 1. Distribution of earthquakes and seismographic stations. a. Location of earthquakes used in the inversion. b. Location of stations.

deep and shallow upper mantle structures (Zhu et al., 2012). Based on a preconditioned conjugate gradient method (Fletcher and Reeves, 1964), we iteratively improve the elastic and anelastic models and gradually reduce the phase and amplitude differences.

2. Dataset and method

2.1. Dataset

In this study, 190 earthquakes recorded by 745 seismographic stations are used to illuminate the crust and upper mantle structure of the European continent and the North Atlantic Ocean (Zhu et al., 2012). Most earthquakes are shallow events with magnitudes ranging from 4.5 to 6.5 and occurring between 1996 and 2011. They are predominantly distributed along the northern Mid-Atlantic Ridge and the Mediterranean–Himalayan Belt. Observed seismograms are collected from the Incorporated Research Institutions for Seismology (IRIS, www.iris.edu), Observatories and Research Facilities for European Seismology (ORFEUS, www.orfeus-eu.org) and the Kandilli Observatory (www.koeri.boun.edu.tr). Additionally, seismic array data from several IRIS/PASSCAL experiments are incorporated in the inversion to constrain local structures, such as underneath Iceland and the Anatolian Plate. Fig. 1 shows the distribution of earthquakes and stations. We have very good data coverage for the upper mantle beneath the European continent and the North Atlantic Ocean. Epicentral distances for our dataset range from a few degrees to more than 60 degrees. A simplified tectonic map of the European continent is shown in Fig. 2, and will be used as a reference for tomographic features discussed in Section 3.

2.2. Starting model

A new 3D crust and upper mantle model of Europe and the North Atlantic Ocean, EU_{30} (Zhu et al., 2012), is used as the starting elastic model. EU_{30} was constructed based on adjoint tomography (Tape et al., 2009, 2010; Zhu et al., 2012). Three-component body and surface waves were combined to constrain radially anisotropic shear wavespeeds throughout the European upper mantle. Thirty preconditioned conjugate gradient iterations (Fletcher and Reeves, 1964) were performed to minimize frequency-dependent phase differences between observed and simulated seismograms, requiring more than 17 100 wavefield simulations and 2.3 million central processing unit core hours. Fig. 3c and d illustrate relative perturbations in vertically and horizontally polarized shear wavespeeds in EU_{30} at a depth of 75 km. In addition, the 1D (radial) shear quality factor Q_μ profile from reference model STW105 (Kustowski et al., 2008a) is chosen as the starting anelastic model (Fig. 3b). Since the bulk quality factor Q_κ is much larger than the shear quality factor Q_μ (Durek and Ekström, 1996), only shear attenuation is considered in this paper. For brevity, in the rest of this paper, we use the symbol Q, rather than Q_μ, to denote the shear quality factor.

2.3. Misfit functions

Phase and amplitude differences between data and synthetics are combined to simultaneously constrain elastic and anelastic structures. Therefore, the total misfit function χ is expressed as

$$\chi = w_\phi \chi^\phi + w_A \chi^A, \tag{1}$$

where χ^ϕ and χ^A are phase and amplitude contributions to the misfit, and w_ϕ and w_A denote corresponding weighting factors, which are used to balance relative contributions of phase and amplitude.

Three-component body and surface waves are combined to simultaneously constrain deep and shallow structures. Therefore, both phase and amplitude misfits in Eq. (1) involve six categories: P-SV body waves on vertical and radial components, SH body waves on transverse components; Rayleigh surface waves on vertical and radial components and Love surface waves on transverse components. For the first iteration, 15–40 s body waves and 40–100 s surface waves are used. As the models and the corresponding synthetic seismograms improve, the corner period of the surface wave measurements is gradually reduced from 40 s to 25 s (for details see Section 2.6).

FLEXWIN (Maggi et al., 2009), an automatic window selection tool, is used to select windows in the data suitable for making phase and amplitude measurements. These windows are selected based on similarities between observed and simulated seismograms. Unlike in classical traveltime tomography, no specific phases, such as P or S, are targeted: any window in which the observed and simulated seismograms are sufficiently close is suitable. A multitaper approach (Laske and Masters, 1996; Ekström et al., 1997; Zhou et al., 2004) is used to quantify frequency-dependent phase and amplitude discrepancies between observed and simulated seismograms in the windows selected by FLEXWIN. In this approach, the phase and amplitude misfits in Eq. (1) may be expressed as